

In summary, a re-examination of the influence of the gas-carbon reaction on the reaction kinetics of FeO by solid carbon using recently available data has shown that this reaction may have a significant effect on the observed rates. A comprehensive mixed control model was used to evaluate the influence of the gas-carbon reaction on the observed reduction rate, and the predictions agree well with the measured data. In general, the overall rate is controlled by the various steps in a series. The predominant step will depend on the stirring condition and type of carbon. The rates observed in graphite are probably not strongly affected by the gas-carbon reaction, the rate limiting steps are liquid phase mass transfer in combination with the slag-gas reaction. On the other hand, when coke is used, the considerably lower reactivity of this carbonaceous material to CO₂ at high temperatures appears to cause this reaction to have significant influence on the rate of reduction.

REFERENCES

1. B. Sarma, A.W. Cramb, and R.J. Fruehan: *Metall. Mater. Trans. B*, 1996, vol. 27B, pp. 717-30.
2. B. Sarma: Ph.D. Thesis, Carnegie Mellon University, Pittsburgh, PA, 1992.
3. S.R. Story and R.J. Fruehan: unpublished research, 1998.
4. E.A. Gulbransen, K.F. Andrew, and F.A. Brassart: *Carbon*, 1965, vol. 2, pp. 421-29.
5. G.R. Belton and R.J. Fruehan: *Proc. Ethem. T. Turkdogan Symp.*, Iron and Steel Society, Pittsburgh, PA, 1994, pp. 3-22.
6. D.R. Sain and G.R. Belton: *Metall. Trans. B*, 1976, vol. 7B, pp. 235-44.
7. D.A. Frank-Kamenetskii: *Diffusion and Heat Transfer in Chemical Kinetics*, 2nd ed. Plenum Press, New York, NY, 1969, pp. 98-109.
8. M. Zamalloa and T.A. Utigard: *Trans. Iron Steel Inst. Jpn.*, 1995, vol. 35 (5), pp. 449-57.
9. S.-H. Liu, R.J. Fruehan, and A. Morales: *Trans. Iron Steel Inst. Jpn. Int.*, in press.
10. S.K. El-Rahaiby, Y. Sasaki, D.R. Gaskell, and G.R. Belton: *Metall. Trans. B*, 1986, vol. 17B, pp. 307-16.

On Optimization of the Powder Plasma Arc Surfacing Process

J.N. DuPONT

The plasma arc welding (PAW) process is frequently used with alloy powder additions for surfacing components subjected to wear and corrosion. Although the deposition rate of this process is typically lower than consumable electrode processes such as gas metal arc welding and submerged arc welding,^[1,2] the ability to independently control arc power and filler metal feed rate generally allows for a higher degree of control over dilution.^[3] Minimizing dilution is important for maintaining the composition, and thus the corrosion/wear resistance, of the weld overlay. As discussed in a recent article,^[3] dilution is minimized by operating the process at a high filler metal feed rate (V_{fm}) to melting power ($\eta_a \eta_m VI$) ratio, where η_a and η_m are the

arc and melting efficiency, respectively, and VI is the arc power. The melting power is simply the fraction of arc power utilized for melting the filler metal and substrate. If the melting power is too low for a given filler metal feed rate, then insufficient power remains to completely fuse the filler alloy to the substrate. In this condition, incomplete fusion can result between the weld overlay and the substrate, which may be susceptible to spallation during service. In addition, the deposition efficiency of the process can be low if insufficient power is available for melting the volumetric feed rate of powder, which is directed to the molten weld pool. (The deposition efficiency is the fraction of total powder that is melted and deposited as part of the weld overlay.) A scheme for controlling dilution has recently been discussed in detail.^[3] In this work, it is demonstrated that the $V_{fm}/\eta_a \eta_m VI$ parameter can also be used for estimating deposition efficiency and fraction of overlay/substrate fusion, F_f .

Figure 1 shows the change in dilution, fraction of overlay/substrate fusion, and deposition efficiency, which are expected to result as the filler metal feed rate is increased for a given melting power. In Figure 1(a) the filler metal feed rate/melting power ratio is low. Only a small portion of the total melting power is required for melting the filler alloy. The remaining power is used by melting a rather large portion of the substrate. Although the deposition efficiency is likely to be high in this condition and there is complete overlay/substrate fusion, the level of dilution is high due to the large quantity of substrate melted. As the filler metal feed rate is increased. (Figure 1(b)), a larger portion of the total power is required for melting the filler alloy and less power is available for melting the substrate. As a result, the quantity of melted substrate decreases, which, in turn, reduces the dilution. Figure 1(b) represents a good balance of parameters because dilution is low while maintaining complete overlay/substrate fusion and a high deposition efficiency. With a further increase in filler metal feed rate (Figure 1(c)), the power available for melting is insufficient to melt all of the filler metal and, in addition, melts little or none of the substrate. At this point, complete overlay/substrate fusion is lost, the deposition efficiency is low, and the critical filler metal feed rate/melting power balance is considered to be exceeded.

It was previously suggested,^[3] but not experimentally verified, that an upper limit could be placed on the maximum filler metal feed/melting power ratio by

$$\frac{V_{fm, \max}}{\eta_a \eta_m VI} = \frac{1}{E_{fm}} \quad [1]$$

where $V_{fm, \max}$ is the maximum volumetric filler metal feed rate and E_{fm} is the melting enthalpy of the filler metal. The value of η_a varies only slightly for a given process, while the melting efficiency can be predicted from knowledge of the arc power and travel speed.^[4,5] Equation [1] simply defines the condition where the filler metal feed rate is at a value where all the melting power would have to be used for melting the filler alloy, in which case no melting power would remain to melt the substrate. This is the condition where the dilution is reduced to an undesirable level of zero and, thus, the value of F_f would also be zero. While this is a simplification of the problem as it does not consider the relative rate of energy transport from the process to the

J.N. DuPONT, Research Scientist and Associate Director, is with the Energy Liaison Program, Lehigh University, Bethlehem, PA 18015.

Manuscript submitted November 24, 1997.

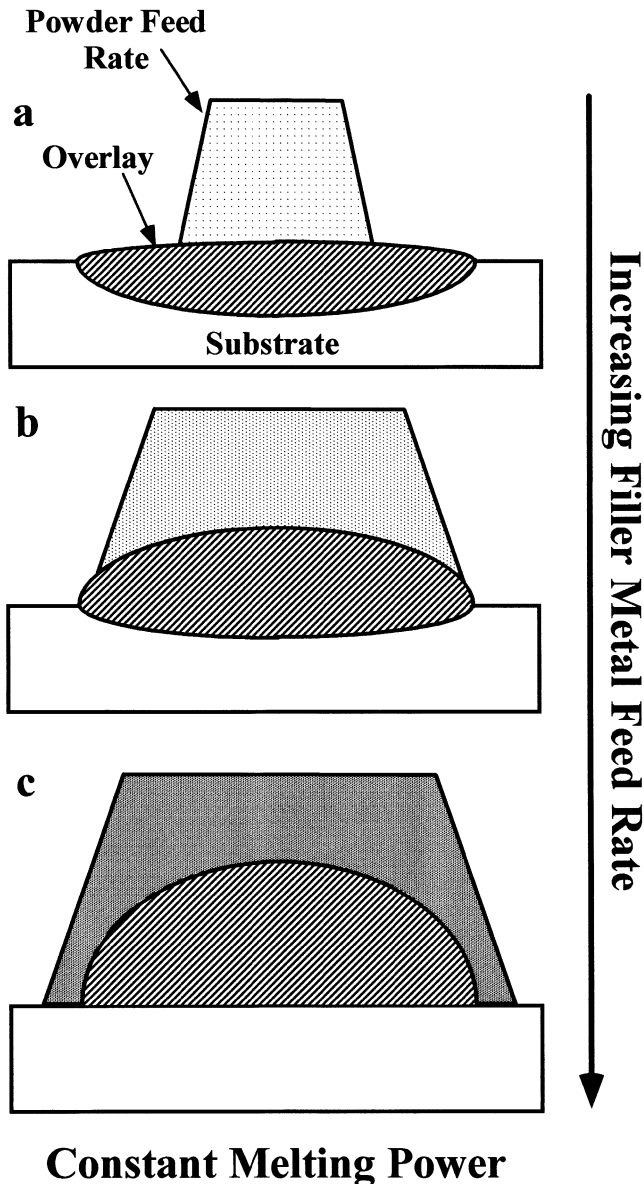


Fig. 1—(a) through (c) Schematic illustration showing variation in dilution, fraction of overlay/substrate fusion, and deposition efficiency with increasing filler metal feed rate at constant melting power.

filler metal and substrate, the condition should provide an upper bound to the limit for the maximum filler metal feed rate.

In this work, the powder PAW process was operated under a wide range of filler metal feed rates and melting powers in order to evaluate the usefulness of Eq.[1] in PAW surfacing applications. The range of parameters was chosen close to the limit of Eq.[1]. The procedure and equipment used was identical to that described previously,^[3,4] where single pass welds were prepared by depositing type 308 austenitic stainless steel powder onto A36 steel substrates. The PAW process was operated using direct current electrode negative polarity with a 4-mm diameter 2 pct thoriated tungsten electrode and argon shielding gas. After welding, each sample was cross sectioned using an abrasive cut-off wheel, polished to a 1- μm finish using silicon carbide paper, and etched in a 2 pct Nital solution. The value of F_f for each condition was measured, as shown schemat-

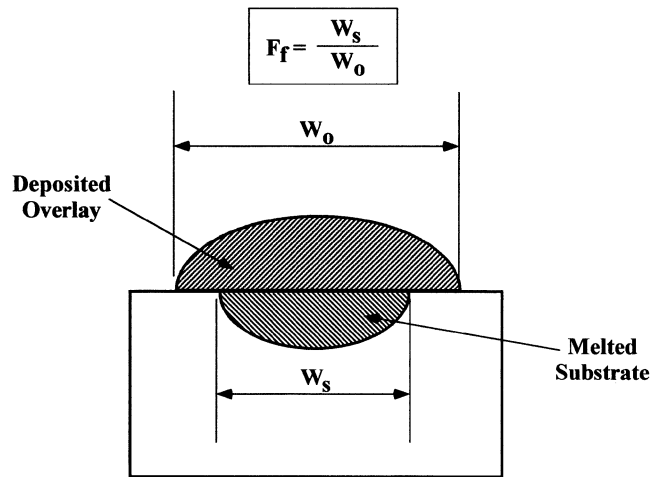


Fig. 2—Schematic illustration showing measurement of fraction of overlay/substrate fusion, F_f .

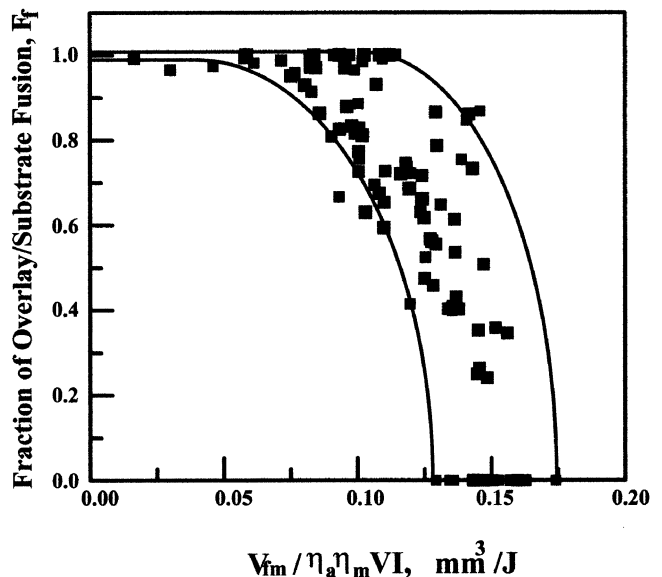


Fig. 3—Fraction of overlay/substrate fusion, F_f , as a function of the filler metal feed rate/melting power ratio.

ically in Figure 2, using a quantitative image analysis system. In three-dimensional space, the value of F_f is defined in terms of the ratio of substrate to overlay melted planar areas at the substrate surface. In practice, when the weld is cross sectioned for examination, these planar areas are reduced by one dimension and are represented by the width of the overlay (W_o) and substrate (W_s) at the substrate surface. This is shown schematically in Figure 2, where the value of F_f is simply defined by the ratio of the width of the melted substrate at the substrate surface, W_s to the width of the melted overlay at the substrate surface, W_o . Thus, when $W_s = W_o$ the overlay is properly fused to the substrate and F_f is equal to unity. The implicit assumption here is that the melted planar areas are constant along the length of the overlay. A similar approach is always taken during dilution measurements.^[3] In three-dimensional space, dilution should actually be defined in terms of the melted volumes of overlay and substrate. However, the melted

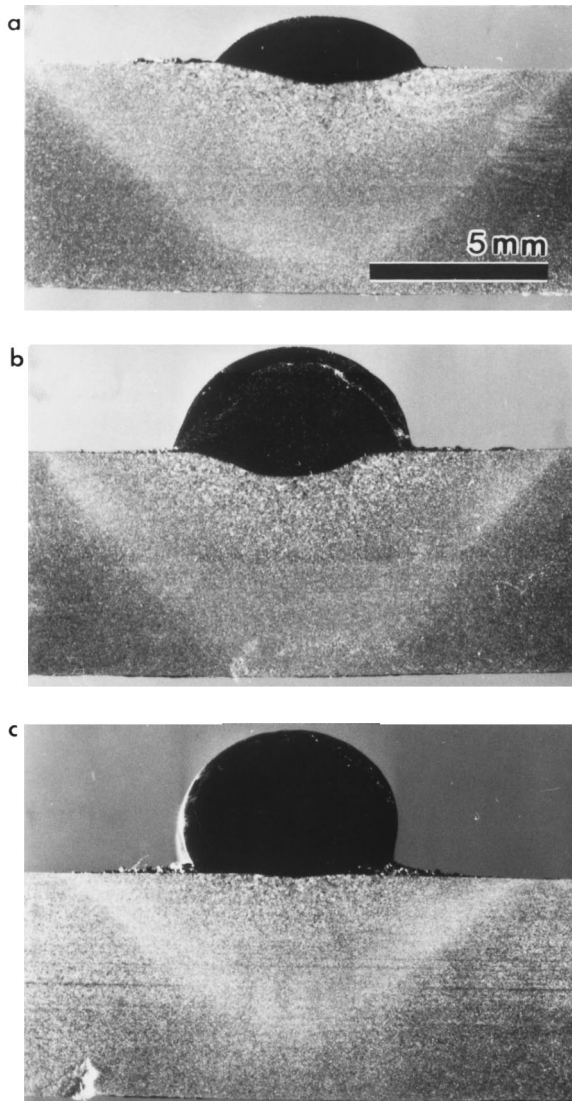


Fig. 4—(a) through (c) Photomicrographs showing decrease in fraction of overlay/substrate fusion as the filler metal feed rate/melting power ratio is increased.

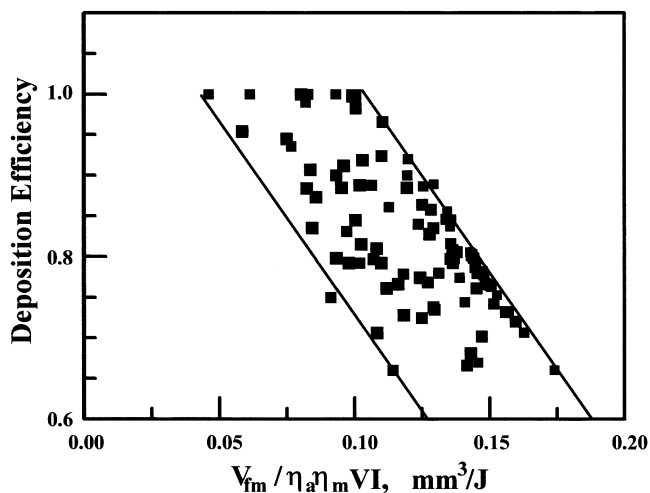


Fig. 5—Deposition efficiency as a function of the filler metal feed rate/melting power ratio.

cross-sectional areas are always used when the weld is cross sectioned and the volumes are reduced by one dimension into areas. The melting efficiency was measured as previously described, and the arc efficiency was assumed constant at 0.47.^[4] The deposition efficiency was determined by measuring the cross-sectional area of deposited overlay and dividing this by the ideal value. The ideal value of deposited cross-sectional overlay is given by the ratio V_{fm}/S , where S is the travel speed.

Figure 3 shows the variation in the fraction of overlay/substrate fusion, F_f , as a function of the $V_{fm}/\eta_a\eta_m VI$ ratio. The gradual decrease in fraction of overlay/substrate fusion with increasing $V_{fm}/\eta_a\eta_m VI$ is shown on several samples in Figure 4. While there is considerable scatter in the data, the results clearly show the trend. The value of $V_{fm}/\eta_a\eta_m VI$, which reduces the overlay/substrate fusion to zero, which should be given approximately by $1/E_{fm} = 0.115 \text{ mm}^3/\text{J}$, is represented reasonably well by the experimental data. (The value of E_{fm} for 308 austenitic stainless steel is 8.7 J/mm^3 .^[6]) Various overlays produced under the critical value of $V_{fm}/\eta_a\eta_m VI$ exhibit an appreciably wide range of overlay/substrate fusion, but still never result in a value of F_f equal to unity. The simple method proposed here cannot account for these variations as it does not consider the relative rate of heat transfer between the filler metal and substrate as it is affected by welding variables. Nevertheless, the simple upper bound analysis provides a useful starting point in the selection of process variables for depositing single-pass overlays with the powder PAW process. Any useful set of parameters must certainly be below the value of $V_{fm}/\eta_a\eta_m VI$ given by Eq. [1], or some incomplete overlay/substrate fusion is likely to result. For this particular set of conditions, the value of $V_{fm}/\eta_a\eta_m VI$ should be below approximately $0.08 \text{ mm}^3/\text{J}$ to maintain F_f levels near unity.

Figure 5 shows the variation in deposition efficiency with the $V_{fm}/\eta_a\eta_m VI$ ratio. Again, there is considerable scatter in the data, but the trend is apparent. As the $V_{fm}/\eta_a\eta_m VI$ ratio increases, less of the incoming powder can be melted and the deposition efficiency decreases. $V_{fm}/\eta_a\eta_m VI$ values below approximately $0.08 \text{ mm}^3/\text{J}$, which produce high overlay/substrate fusion levels, lead to deposition efficiency levels above 0.8. These concepts, when combined with the previous method outlined for controlling dilution,^[3] should be useful for selecting optimized parameters for the plasma arc surfacing process.

REFERENCES

1. H. Hallen, A. Lugscheider, and A. Ait-Mekideche: *Proc. 4th National Thermal Spray Conf.*, Pittsburgh, PA, 1991, pp. 537-39.
2. R.S. Chandel: *Weld. J.*, 1987, vol. 66, pp. 135s-140s.
3. J.N. DuPont and A.R. Marder: *Metall. Mater. Trans. B*, 1996, vol. 27B, pp. 481-89.
4. J.N. DuPont and A.R. Marder: *Weld. J.*, 1995, vol. 74 (12), pp. 406s-416s.
5. P.W. Fuerschbach and G.A. Knorovsky: *Weld. J.*, 1991, vol. 70 (11), pp. 287s-297s.
6. C.F. Lucks and H.W. Deem: *Thermal Properties of Thirteen Metals*, ASTM STP No. 227, ASTM, Philadelphia, PA, 1958.